Optical Spectroscopy of Marine Bioadhesive Interfaces*

Daniel E. Barlow and Kathryn J. Wahl

Chemistry Division, U.S. Naval Research Laboratory, Washington, DC 20375-5342

Annu. Rev. Anal. Chem. 2012. 5:229–51

First published online as a Review in Advance on April 9, 2012

The *Annual Review of Analytical Chemistry* is online at anchem.annualreviews.org

This article's doi:
10.1146/annurev-anchem-061010-113844

1936-1327/12/0719-0229$20.00

Keywords

in situ spectroscopy, infrared, Raman, biofouling, attenuated total reflectance

Abstract

Marine organisms have evolved extraordinarily effective adhesives that cure underwater and resist degradation. These underwater adhesives differ dramatically in structure and function and are composed of multiple proteins assembled into functional composites. The processes by which these bioadhesives cure—conformational changes, dehydration, polymerization, and cross-linking—are challenging to quantify because they occur not only underwater but also in a buried interface between the substrate and the organism. In this review, we highlight interfacial optical spectroscopy approaches that can reveal the biochemical processes and structure of marine bioadhesives, with particular emphasis on macrofoulers such as barnacles and mussels.

1. INTRODUCTION

A wide variety of organisms in nature use highly adapted processes to attach temporarily or permanently to surfaces. This process is known as bioadhesion, and it plays a vital role in organisms' life cycles and survival (1). Interdisciplinary efforts to understand bioadhesion are increasing, spanning the disciplines of biology, chemistry, physics, and engineering. These efforts stem from the need to prevent unwanted bioadhesion, referred to as biofouling, as well as from interest in replicating bioadhesion. In the marine environment, sessile organisms that permanently adhere to surfaces range from microscopic (i.e., algae, bacteria, and diatoms) to macroscopic (i.e., mussels, barnacles, and tubeworms). Biofouling by these organisms is an immense problem for maritime shipping and industry and costs billions of dollars per year in preventative surface treatments, repair, and removal; it also leads to increased shipping fuel costs from added drag. Understanding how these organisms adhere is also of interest for applications such as biologically compatible surgical adhesives that can bond to wet surfaces. This review focuses on optical spectroscopies applied to marine bioadhesion.

Adhesion of marine organisms to substrates is a complex, often multistage, process (1, 2). Permanent marine bioadhesion typically begins with motile organisms in a swimming stage. For example, algal species such as *Ulva* spp. have swimming sporelings, whereas mussels, oysters, and barnacles have larvae. All are capable of substrate probing and settlement, which can be influenced by various factors such as biochemical signaling (3) and substrate properties (4–7). Larval surface exploration may also involve the release of temporary adhesive (8). Fundamental questions about the permanent adhesive interface include both the composition and the chemical structure of the adhesive layer, as well as the chemical processes and kinetics involved. The initiation of polymerization and cross-linking, which are properties of the cohesive and adhesive interactions, and exclusion of water from the interface are also relevant. Marine organisms successfully adhere to substrates with a wide range of compositions and surface properties, including preexisting biofilms from other organisms, under widely varying environmental conditions.

2. METHODS TO EVALUATE THE CHEMISTRY OF ADHESIVES IN BIOINTERFACES

No single analytical method can fully describe a material's interfacial chemistry and structure. This is especially true for biointerfaces, which are typically highly complex structures that often contain both organic and inorganic components. Therefore, experimental approaches to understanding bioadhesion require the use of multiple complementary methods. Berglin et al. (9) have previously reviewed many analytical methods that are useful in characterizing the adsorption and cross-linking of marine bioadhesives, including attenuated total reflectance Fourier transform infrared (ATR-FTIR) spectroscopy, X-ray photoelectron spectroscopy (XPS), ellipsometry, quartz crystal microbalance with dissipation monitoring, and surface plasmon resonance (SPR) as surface-sensitive methods, as well as bulk methods such as nuclear magnetic resonance (NMR), matrix-assisted laser desorption/ionization time-of-flight mass spectrometry (MALDI TOF MS), and protein separation by gel electrophoresis. Atomic force microscopy (AFM) has also been used by many groups to examine the adsorption, structure, and mechanical properties of marine adhesives (10–14).

To date, many studies of marine bioadhesion employ ex situ methods to understand the biochemical composition of marine bioadhesives. One example in which ex situ biochemical studies have succeeded is the identification of (3,4-dihydroxyphenyl)-L-alanine (DOPA), which is a modified tyrosine containing an additional −OH on the phenyl ring as a key cross-linking and

adhesive substituent in mussel cement (15). This success led to the continuing exploration of DOPA-functionalized materials for biomaterial development and adhesive applications (16, 17). Methods have also been reported for the collection of unpolymerized barnacle cement (13, 18–21). Naïvely, one might think that this material could be applied to two surfaces that would show adhesion similar to that of the barnacle. So far, such a similarity has not been demonstrated. To reveal the chemical processes and complexities by which marine macrofouling organisms achieve robust adhesion, it will be necessary to develop approaches to directly analyze the naturally formed adhesives and adhesive interfaces. Methods for which this can be done in situ to probe the buried interfaces of live organisms are of particular interest.

In this review, we highlight the many important advantages offered by linear optical spectroscopies such as FTIR, Raman, and circular dichroism (CD) that make them productive experimental methods for marine bioadhesion studies. Further, we emphasize the importance of in situ experimental configurations, where possible, to probe buried adhesive interfaces. Through the careful selection of instrument configuration and sample preparation, many chemical aspects and processes that influence bioadhesion can be examined. The opportunity to conduct real-time characterization of chemical composition, structure, adsorption, and other time-dependent changes at buried adhesive interfaces of live organisms is particularly exciting (22–24). Vibrational spectroscopies are directly sensitive to chemical composition, bonding, and geometric structure, often providing unique chemical fingerprints of samples. At surfaces and interfaces, vibrational spectroscopies are also extensively used to probe molecular orientation. Long-range vibrational coupling can also provide information about larger-scale structure, particularly protein secondary structure (25). CD is another method employed for this purpose, although solid-state CD has not yet been widely adopted. An important nonlinear spectroscopy that also deserves mention is sum-frequency generation. This technique is not covered here but has been reviewed by Le Clair et al. (26) for bioadhesion studies. Interpretation of optical spectra can be more complex than with other common methods, but with careful analysis, complementary experiments, and/or theoretical calculations, they can be powerful methods for characterizing biointerfaces.

3. STRATEGIES FOR SAMPLE COLLECTION AND PREPARATION

Because marine bioadhesion involves live organisms and typically a thin adhesive interface, some thought must be put into reliably obtaining and preparing samples for analysis. Although purified mussel adhesive proteins can be obtained commercially, most other marine organisms, including barnacles, require that adhesive be obtained directly from the organism. The most straightforward approach for barnacles and other hard foulants has been to dislodge them from various substrates and analyze the material remaining on the substrate (27). Doing so is usually difficult because macrofoulers such as barnacles can strongly adhere to most substrates (28), although silicone-based coatings are a notable exception and are widely used as foulant-release coatings on commercial ships.

Our laboratory's work on marine bioadhesion has focused primarily on acorn barnacles, specifically *Balanus amphitrite*. A barnacle of this species adheres by proteinaceous secretions that cure under its protective shell. The barnacle enlarges its shell by adding calcified material to the bottom of a set of interconnected side (parietal) plates and growing upward while expanding the base from the periphery. The adhesive is secreted from structures in the baseplate and does not extend beyond the growing edge of the barnacle. The dried adhesive layer of *Balanus amphitrite* is typically approximately 600 nm thick and may be several micrometers thick underneath a live barnacle. On certain substrates (particularly foulant-release materials such as silicones), barnacles may produce concave bases filled with an opaque, tacky substance referred to as a gummy adhesive (29–31). It

is not known exactly how this material differs from normally cured adhesive, although it contains many of the same biochemical components (32).

Solution-state evaluation by biochemical methods has revealed the amino acid composition of barnacle cement, as well as the presence of several proteins (33–36). Kamino and coworkers (37) showed that barnacle cement proteins are partially solubilized by the strong protein denaturant guanidine HCl; only in the added presence of the strong reducing agent DTT (dithiothreitol) at high concentration (0.5 M) were most of the remaining proteins solubilized. Although denaturing has enabled the identification of the adhesive proteins and amino acid compositions, the curing chemistries and nature of the protein structure were not identified. However, direct ex situ, in situ, and even in vivo analyses of intact adhesive proteins are possible with optical probes such as FTIR and Raman spectroscopies.

We use the barnacle as an example to provide an overview of sample-preparation approaches for interfacial analysis. An advantage of the methods described in this review is that they utilize inexpensive commercial spectrometers that require minimal technical skill to operate. The key to obtaining high-quality interfacial data is in devising sample-preparation strategies for interfacial analysis and coupling the spectrometer to the appropriate optical configuration. **Figure 1** presents three types of sample preparation for direct observation of barnacle adhesive with optical spectroscopy—two ex situ and one in situ/in vivo method. The ex situ methods also provide samples suitable for additional evaluation by other physical chemistry and materials analysis tools such as AFM, nanoindentation, and optical interferometry.

Raman and FTIR experiments can be performed in transmission mode through appropriate substrates [e.g., glass or sapphire for Raman, and silicon (Si), germanium (Ge), or CaF_2 for FTIR]. Barnacles can be transferred to these substrates from silicone-coated release panels or reared directly on substrates by settling cyprids. The adhesive protein matrix can be examined ex situ following decalcification with EDTA (ethylenediaminetetraacetic acid) or dilute HCl. More importantly, direct in situ and in vivo analyses of intact bioadhesive interfaces can be accomplished through the use of reflectance techniques with Raman or FTIR optics.

4. FOURIER TRANSFORM INFRARED SPECTROSCOPY

FTIR spectroscopy is among the most widely used instrumental methods in analytical chemistry. FTIR offers the advantages of common instrumentation availability, low cost, minimal technical ability to operate, and nondestructive sample analysis. Also, FTIR can be configured to characterize virtually any type of interface in various environments (i.e., vacuum, gas, liquid); other surface

Figure 1

Overview of sample-preparation strategies for optical spectroscopies, including Fourier transform infrared (FTIR), Raman, and circular dichroism (CD). Three major sample-preparation approaches are shown. For all experiments, the barnacles are first reared from the cyprid stage to maturity by settling on either temporary (silicone release coatings) or permanent (e.g., quartz, CaF_2, Ge, Si) substrates. For ex situ analysis of the adhesive, the upper portion of the barnacle can be removed and the cement examined in transmission following decalcification to remove the baseplate. Alternatively, barnacles reared on silicones can be carefully removed and reattached to the desired optical substrate. After some time (say, 30–70 h), the barnacles will have secreted adhesive; by removing the barnacles at this stage, one can examine the cement deposited during the reattachment stage. Finally, the intact interface can be examined by reflectance geometries, including Raman microscopy and attenuated total reflectance (ATR) infrared spectroscopy. ATR geometry provides additional surface sensitivity to chemistries within the near field (within 1 μm) of the surface. When the barnacles are reared on doubly polished substrates with optical properties that are identical to those of the ATR crystal, the reflected beam can be brought directly to the barnacle adhesive. This process enables in situ (intact) or in vivo (of the live organism) spectroscopic access to the interface. Abbreviation: AFM, atomic force microscopy.

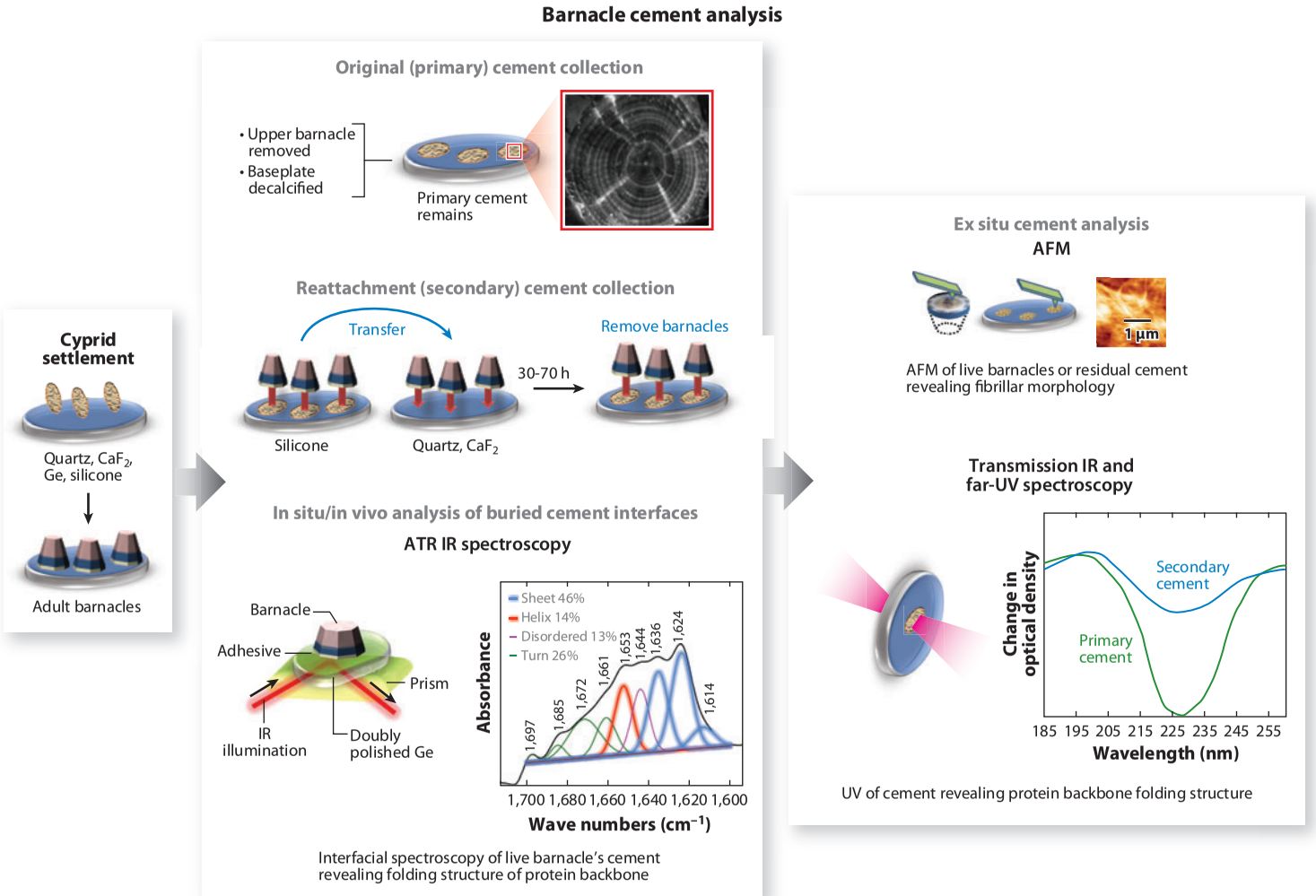

analytical methods are often limited in this aspect. Although many types of optical configurations have been devised for different types of sample analysis with FTIR (38), the analyses described here use either single-pass transmission or ATR.

FTIR offers sufficient sensitivity to detect submonolayer surface spectra, although it is not an inherently surface-sensitive technique. FTIR generally requires initial collection of a reference spectrum without the analyte present; the reference component is then removed from the analyte component in subsequent sample spectra. The collection of high-quality absorption spectra therefore necessitates that the reference and sample spectra be collected under nearly identical conditions. In situ ATR-FTIR experiments offer the advantage of preserving the optical path if the internal reflectance element is maintained in the same position for collection of reference and sample spectra. Good temperature stability is also necessary to ensure that thermal expansion or contraction does not alter the optical path; temperature instability effects can cause miscancellation of background features and obscure the true detection limits of the instrument. Temperature control of ATR elements may also be required for in situ experiments with live organisms (23). Also, atmospheric water vapor and CO_2 strongly absorb in the mid-IR range and must be maintained at low constant levels, usually by nitrogen purge. Because water vapor bands are of a much narrower width than the solid- or liquid-phase bands being analyzed, they can easily be observed superimposed on the broader bands, if not completely canceled. Such unwanted signals are amplified by resolution-enhancement methods such as Fourier self-deconvolution (FSD). Elimination of water vapor bands is especially important in analyses of absorption spectra between 1,500 and 1,750 cm^{-1}, an important region for biopolymer analysis. Methods have been developed to remove water vapor bands, but in the ideal experiment these bands are not present in the first place. CO_2 can be used to "leak test" spectrometer seals by monitoring CO_2 absorption at 2,300–2,400 cm^{-1} in real time. Attaching a nitrogen-purged glove bag over the spectrometer sample compartment can also improve the nitrogen purge during data acquisition and sample exchange. In detailed analyses, it is good practice to compare the data with a water vapor spectrum acquired at the same resolution to avoid incorrect assignment of water bands.

The composition and the biochemical structure of natural marine bioadhesives are readily revealed by vibrational spectroscopy (38). Easily identifiable compositional features in FTIR spectra include those of minerals, biopolymers, and water. Amino acid side chains may also be identifiable to various degrees (39). Phenolic functional groups such as tyrosine and DOPA are readily distinguishable by FTIR and play key roles in bioadhesion (40–42). Raman spectroscopy is often more effective in identifying side chains (see Section 5). Because hard marine foulants typically have calcerous shells, $CaCO_3$ is among the top mineral components found in IR spectra of their adhesives (42, 43). Diatoms, by contrast, have a high silica content (44). Different types of biopolymers are usually observed in both temporary and permanent bioadhesives; these include proteins (42), glycoproteins (23), and polysaccharides (22, 45); sulfated (23, 44) and phosphorylated versions of these polymers; and DNA (46). In addition to adhesion biochemistry, substrate chemical changes facilitated by bioadhesion may also be studied by FTIR, as in studies of corrosion (47). Complementary methods for compositional analysis, such as XPS and energy-dispersive X-ray (EDX) analysis, are often very useful in assigning IR bands to various chemical functionalities (23, 24, 44) and allow the chemical properties of biomaterials to be explored in greater detail by use of FTIR.

Once the basic compositional characteristics of a bioadhesive interface are determined, further biochemical details such as protein secondary structure can also be explored by FTIR. The most common method for identifying protein secondary structure by FTIR is by analysis of the amide I/I′ band (amide I′ indicates deuterium exchange in D_2O). A widely used approach was developed by Byler & Susi (48); it uses deconvolution methods to resolve overlapping bands. Deconvolution

of spectroscopic protein structure data is generally applied to the characterization of single, purified proteins, but it has also been used for unprocessed marine bioadhesives that are mostly proteinaceous, such as barnacle cement (10, 14, 42). Proteins exhibiting β-sheet structure generally have maxima between 1,620 and 1,640 cm^{-1}, whereas α-helical structures display maxima near 1,654 cm^{-1} (25, 48). Protonated disordered structures also absorb near 1,654 cm^{-1}, and the liquid water bending mode appears near 1,640 cm^{-1}. Deuteration of the sample in D_2O can facilitate more reliable analyses by shifting the disordered absorbance to ∼1,645 cm^{-1} and the water bending mode to 1,208 cm^{-1} (25). Another important protein structure found frequently in marine adhesives and other biomaterials is amyloid (10, 14, 49–51), which has a distinctive signature in the IR that generally consists of a sharper, lower-frequency amide I band at 1,610–1,630 cm^{-1} (52). Other important characteristics of marine bioadhesives that have been characterized by FTIR include cross-linking (41, 53). Many types of experiments can also be done in situ with FTIR spectroscopy; even the time-dependent formation of buried adhesive interfaces of live organisms can be characterized (22, 23). Examples of FTIR analysis applied to marine bioadhesives are given in the following subsections.

4.1. Ex Situ Analysis of Barnacle Adhesive Interfaces

As with other analyses of marine bioadhesives, most FTIR analyses of barnacle cement have been ex situ. Some of these reports have analyzed cement scraped from dislodged barnacles and prepared in KBr pellets (43, 47, 54). These analyses generally confirmed the proteinaceous nature of the cement and revealed variations in cement composition and structure for barnacles grown on different substrates. Alternate approaches have also been used to examine the adhesive ex situ while avoiding the difficulties sometimes encountered in dislodging barnacles and manually collecting only the adhesive. Both Sullan et al. (14) and Barlow et al. (10) used the scheme shown in **Figure 1** for secondary cement collection, which allowed barnacle cement to be collected on CaF_2 substrates. The reattached barnacles were removed before they became strongly adhered, which left cement on the substrates for analysis by transmission FTIR. Barlow et al. used the same scheme to isolate native cement on CaF_2 substrates for comparison with the reattached barnacle cement. These studies focused on analysis of either the amide I or amide I′ (after D_2O exchange) bands for estimation of the protein secondary structure through the use of FSD and peak fitting (**Figure 2**). Sullan et al. (14) identified one major peak assigned to random coil structure and three minor peaks assigned to β-sheet structure. Barlow et al. (10) showed that both of the primary and secondary cement interfaces had similar protein secondary structure components. In this analysis, the major component was β-sheet structure; minor contributions were from α-helix, turn, and disordered structures. Additional details from the amide I′ analysis of the FTIR results showed that the β-sheet structures consisted of both globular and amyloid cross-β-sheet components. The cross-β-sheet component was estimated to be 22% to 28%. Given that the cross-β-sheet components of pure amyloids are reported to range from 35% to 80% (52, 55), the amyloid content in barnacle cement may be ∼20% or higher. AFM images of barnacle cement showed that these samples were composed largely of nanoscale fibrils with diameters as small as ∼2 nm, which is also consistent with the presence of amyloid.

4.2 In Situ Analysis of Marine Bioadhesive Interfaces

Despite the merits of rigorous ex situ analysis of adhesive proteins, it is desirable to evaluate whether the information obtained from those studies reflects the chemistry in the intact interface. One advantage of vibrational spectroscopies for marine bioadhesion studies is the ability to characterize

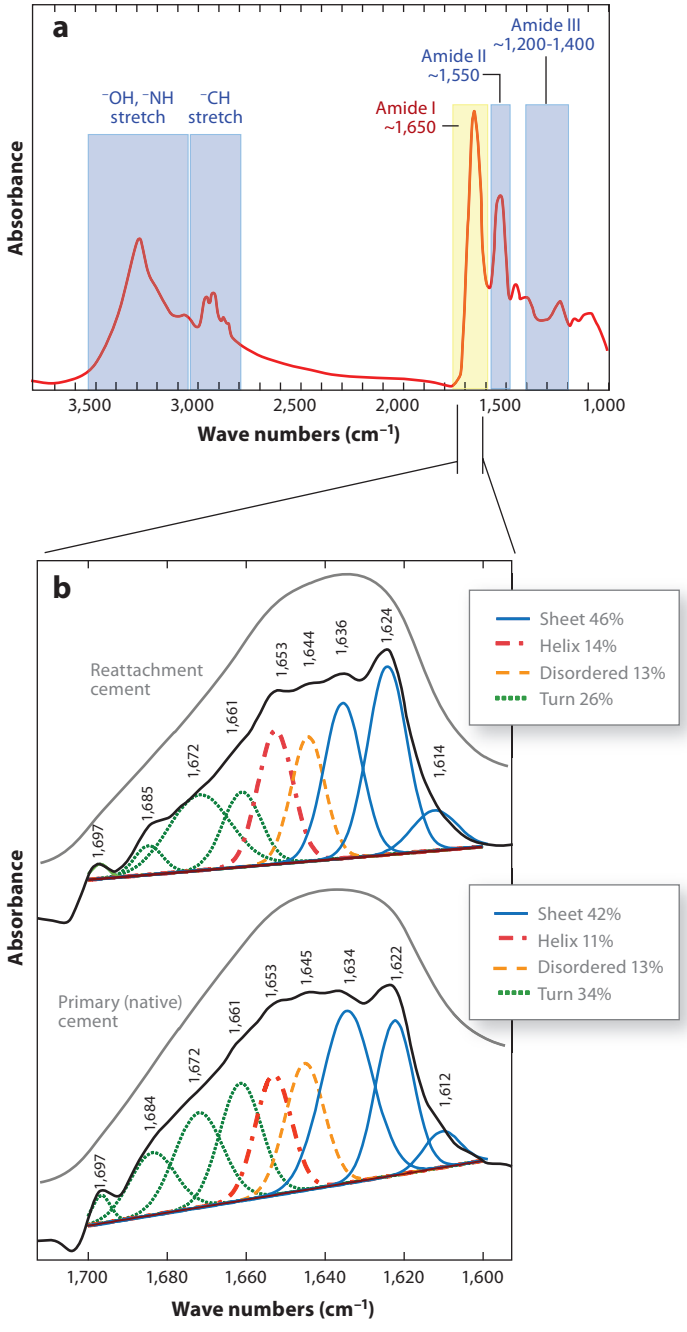

Figure 2

(*a*) Transmission Fourier transform infrared (FTIR) spectrum of reattached barnacle cement through CaF_2 (*inset*) under dry N_2. Various spectroscopic regions of interest for biological materials are highlighted. (*b*) Amide I′ (*yellow region in panel* a) FTIR spectra of native (*upper*) and reattachment (*lower*) cements obtained in transmission. The gray curves show the original spectra, and the black curve shows the spectra following resolution enhancement by Fourier self-deconvolution. The results of peak fitting are shown by color-coded curves. Adapted in part from Reference 10.

buried adhesive interfaces of live organisms. Although spectra of live organism adhesive interfaces can be difficult to interpret, virtually all aspects of the real adhesive interface can be captured without risk of misdiagnosis due to modifications that occur with ex situ diagnosis or simplified model studies. Further, real-time studies of bioadhesion can capture all the processes of interest: from adsorption processes to water displacement, adhesion, and cohesion processes. In cases in which real-time in vivo studies are overly complicated, simplified model characterizations can also be performed and compared with the in vivo data to verify the validity of the proposed model. Wetting, or the effects of surface conditioning agents that play roles in bioadhesion but do not permanently adsorb, may also be monitored.

4.2.1. The attenuated total reflectance configuration. The ATR configuration is the most widely used for in situ FTIR spectroscopy. Within the ATR-FTIR configuration, there are numerous ways to design an experiment (38), some of which are outlined in **Figure 3**. In the simplest

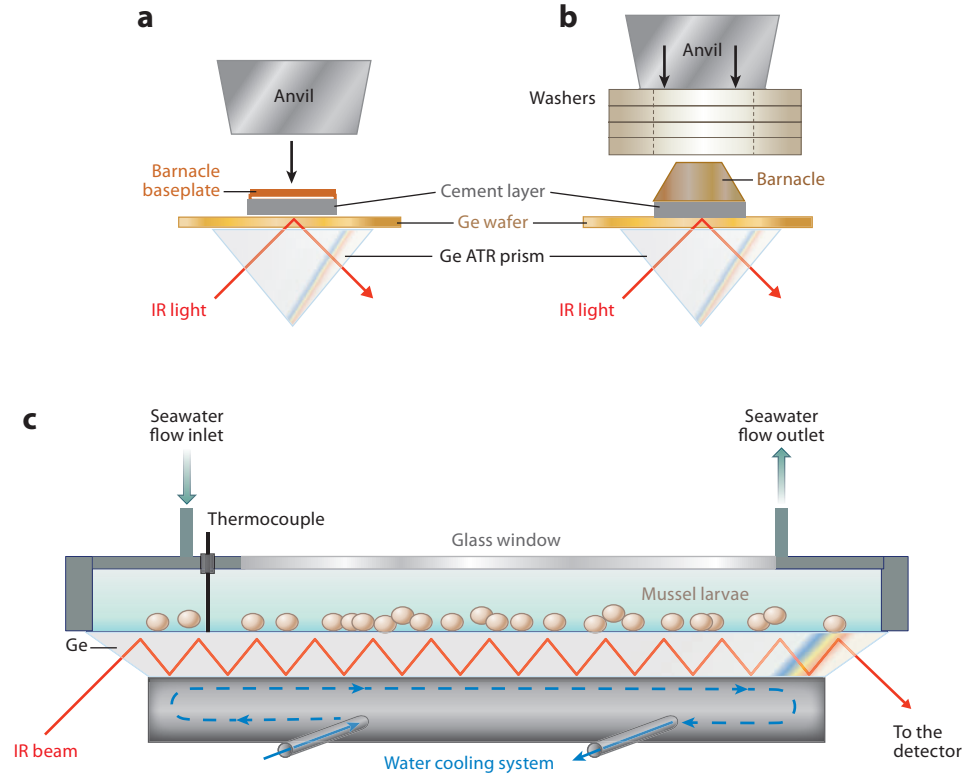

Figure 3

Examples of attenuated total reflectance (ATR) experimental geometries for marine bioadhesive experiments. (*a*) Barnacle grown on a doubly polished Ge wafer; the barnacle body has been removed, and the calcified structures are intact. In this configuration, the anvil can press directly on the upper side of the baseplate to obtain good transmission through the Ge interfaces. (*b*) In vivo experiments on live organisms can also be performed through the Ge wafer interface. To obtain good contact between the Ge ATR prism and the Ge wafer, a set of washers can be used to carefully compress the Ge surfaces together while allowing the organism to remain hydrated if desired. (*c*) The configuration used by Petrone et al. (23) is a multiple–internal reflection element ATR prism. A flow cell was mounted between the prism and a glass plate and sealed with o-rings. Adapted from References 23 and 42.

Table 1 Refractive indices and calculated penetration depths at 1,000/1,500/3,000 cm^{-1} for $n_2 = 1.5$

Reflection element	Refractive index, n_1	Penetration depth (μm); $d_p(\theta = 45°)$	Penetration depth; $d_p(\theta = 60°)$
Ge	4.0	0.66/0.44/0.22	0.48/0.32/0.16
ZnSe, diamond	2.4	2.01/1.34/0.67	1.01/0.67/0.34

form, IR light is directed through a triangular prism and is internally reflected at the top surface (**Figure 3*a***). Internal reflection occurs when the angle of incidence, θ, is above the critical angle, given by $\theta_c = \sin^{-1}(n_2/n_1)$, where n_1 and n_2 are the refractive indices of the internal reflection element and the sample, respectively. Upon internal reflection, an evanescent wave decays exponentially into the sample side of the interface, allowing this region to be probed spectroscopically. Sensitivity is highest at the interface, and the degree to which sensitivity decays beyond the interface is typically indicated by the penetration depth, d_p. This value refers to the distance at which the evanescent wave has decayed to $1/e$ of the intensity at the interface:

$$d_p = \frac{\lambda}{2\pi n_1 \sqrt{\sin^2\theta - \left(\frac{n_2}{n_1}\right)^2}}. \quad (1)$$

Thus, the penetration depth depends on the wavelength, the angle of incidence, and the refractive indices of the prism and sample. **Table 1** lists data for materials commonly used in internal reflection elements. Note that the wavelength dependence of the penetration depth also results in diminished absorption intensities at higher frequencies. Most commercial FTIR software offers a correction to approximate the true relative intensities for a pseudoconstant penetration depth.

Ge is the material with the highest index of refraction in the mid-IR range; it offers the lowest penetration depth range and the highest sensitivity at the interface. Variable-angle ATR can be used for depth profiling with hemispherical elements. In addition to single-reflection ATR prisms, multiple–internal reflection prisms may also be used. These extend the effective path length and increase analyte sensitivity (38).

ATR-FTIR can also be performed with coated internal reflectance elements to examine chemical interactions on other surface compositions, so long as the coating is thinner than the penetration depth. Any type of coating may be applied, including organic materials, metals, and oxides. If the coating is composed of nanoparticles or is porous, it provides the advantage of additional surface area within the sampling volume (24, 56). One issue in working with aqueous samples for FTIR spectroscopy is that water is strongly IR absorbing. However, excessive light attenuation by water is generally not an issue in the ATR configuration, except for some cases in which long–path length internal reflection elements are used with higher penetration depths. Other factors that can affect ATR-FTIR intensities include changes in sample density, such as with hydration-dependent swelling or collapsing, or changes in the overall refractive index at the interface (53). In situ ATR-FTIR experiments of marine sessile organisms have focused primarily on mussels (23, 53) but also include recent reports on barnacles (42) and kelp spores (24).

4.2.2. Barnacles. Barlow et al. (42) applied ATR-FTIR spectroscopy in a unique way to characterize the buried, undisturbed adhesive interfaces of adult barnacles. This method allowed for collection of reference spectra and analysis of multiple specimens under different conditions, all done on the same ATR prism without disruption to the optical path. Barnacle cyprids were first settled onto double-side-polished Ge wafers and then raised to adults over a period of at least

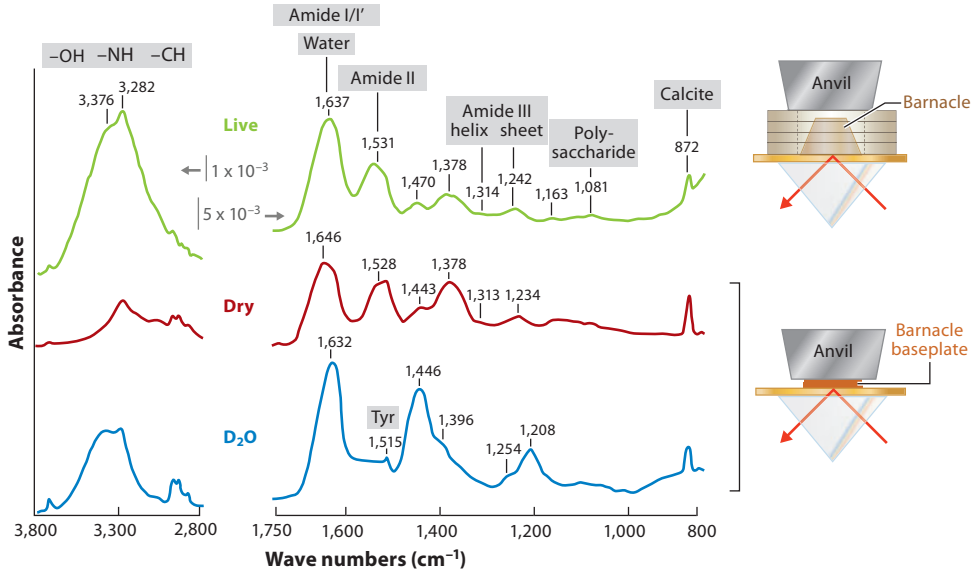

Figure 4

Comparisons between averaged ATR-FTIR (attenuated total reflectance Fourier transform infrared) spectra of barnacle cement interfaces on Ge substrates under different preparation conditions. Maxima of selected peaks and shoulders are identified, and the right-hand portions of the spectra have been enhanced by a factor of five, as noted. The top spectrum (*green*) was averaged from a live barnacle interface obtained in the specimen geometry shown at the upper right. After removal of the barnacle (but with the baseplate intact) and drying in an N_2 atmosphere, the middle (*red*) averaged spectrum was obtained. The lower (*blue*) spectrum was obtained for the barnacle baseplate in D_2O. Adapted from Reference 42.

two months. These specimens were determined to represent cases of robust, defect-free adhesion with hard cement interfaces approximately 600 nm thick. ATR-FTIR analysis was done without any disruption to the adhesive interface by pressing the wafer holding the barnacle onto a single-bounce Ge ATR prism (**Figure 3*b***). Either a protective stack of washers or a hollow, machined cylinder was placed over the barnacle and then pressed with an anvil to achieve good wafer-prism contact. The IR light then transmitted through the Ge wafer–Ge prism interface and internally reflected at the barnacle-wafer interface for spectroscopic analysis. Note that ATR elements with lower refractive indexes, such as ZnSe, can also be used with Ge wafers. Such an arrangement should result in improvements due to better light transmission into the wafer.

Another useful approach we developed (42) was to analyze the adhesive interface after removing the upper portion of the barnacle body and shells, leaving the strongly adhered $CaCO_3$ baseplate behind. We obtained better wafer-prism contact by pressing directly on the barnacle baseplate with the anvil. In comparison to those from live barnacle analysis, spectra of the interface acquired immediately after removal of the upper portion of the barnacle were identical. Working with the adhered baseplate also allowed analysis of the interface under different conditions, for example, baseplate interfaces acquired after dehydration in dry nitrogen and deuterium exchange in D_2O.

Figure 4 shows spectra for wet, dry, and deuterated interfaces. **Figure 4*a*** shows that the original interface is mostly proteinaceous, as indicated by the dominant amide I and II bands near 1,637 and 1,531 cm^{-1}. Some polysaccharide was also present, as indicated by the small peak at 1,081 cm^{-1}, in agreement with previous biochemical analyses (57). Calcium carbonate was a minor component, as indicated by the sharp peak at 872 cm^{-1}, but most of the signal was attributed to

$CaCO_3$ at the baseplate rather than in the proteinaceous cement layer. The water content in the hard cement of live barnacles was estimated at 20% to 50% by weight. Reliable measurement of the water content from the original interface is important for understanding the role of water displacement in bioadhesion. In comparison, gummy barnacle cement, which can be obtained in much larger quantities, contains up to 87% water by weight (58). These differences correlate with robust and problematic adhesion, respectively. Exposure of baseplate interfaces to dry nitrogen for 48 h at ambient temperature removed nearly all the water, as indicated by the absence of the −OH stretching band, which demonstrates that water is weakly bound. Deuterium exchange occurred readily, as identified by the typical displacement of the amide II band. Further details of the biochemical structure were extracted by analyzing the amide I′ band following deuterium exchange to estimate the protein secondary structure content. As in the ex situ study, this analysis revealed that β-sheet was the most prominent secondary structure; α-helix and disordered structures were also present.

4.2.3. Mussels. To date, the McQuillan group (22, 23) has published two studies examining the original adhesive interfaces of macrofouling organisms. These studies were real-time analyses of juvenile mussels and mussel larvae adhering in seawater within a flow cell. The first of these studies characterized the real-time adhesion of live juvenile mussels (*Mytilus galloprovincialis* and *Perna canaliculus*) to ZnSe and TiO_2-coated ZnSe prisms. Two main adhesive secretions were distinguished: the permanent adhesive from the byssus (attachment) threads and a temporary adhesive from the foot organ, which aids movement for surface exploration. Background spectra were collected with seawater flowing through the cell. Then either freshly collected mussels or stored mussels were placed on the prism, and absorbance spectra were collected over time to monitor mussel adhesion. Spectra were also collected of residues on prism substrates after mussel removal and rinsing, which allowed permanently adhered components to be distinguished from those that were temporarily adsorbed. Permanently adsorbed components were consistent with protein, and peaks corresponding to lipid ester and phosphodiester functionalities were also observed. Interestingly, the spectra of permanently adsorbed material were similar for both freshly collected and aged mussels, whereas significant differences were observed in the real-time spectra. Much greater movement of the stored mussels was observed following settlement on the ATR prism, and the time-dependent spectra were consistent with the presence of mucopolysaccharide, which is secreted from mussel foot glands to facilitate movement. Negative IR absorbances observed near 1,670 cm^{-1} in real-time spectra were attributed to possible displacement of water by adsorbed mussel adhesive materials. Mussel bioadhesion on TiO_2-coated prisms was done specifically to aid the detection of catechol binding from DOPA because catechols are known to bind strongly to TiO_2. Notably, the authors concluded that catechol detection was not supported by the results.

Mussel settlement on the ATR prisms required chilled (~16°C) water. The experiments were complicated by elevated temperatures at the surface due to restricted water flow when mussels were placed on the prism surface within the flow cell. The investigators solved this problem by using a modified flow cell with a metal cooling block beneath the trapezoidal ATR prism to maintain constant temperature (23). Although most studies of mussel adhesion have focused on the adult phase, the study by Petrone et al. (23) examined primary settlement of *P. canaliculus* mussel larvae at the pediveliger stage, when the organisms do not yet produce DOPA (**Figure 5*a***). The spectra were consistent with the presence of glycoproteins. **Figure 5*a*** shows spectra for 18- and 25-day-old larvae collected immediately after the larvae settled on the prism surface. These spectra are referenced to seawater. The peaks near 1,652 cm^{-1} and 1,547 cm^{-1} were assigned to the typical amide I and amide II peaks of proteins, and the 1,520 cm^{-1} peak was assigned to ring modes of aromatic groups. The position of the amide I band was attributed to α-helix as a

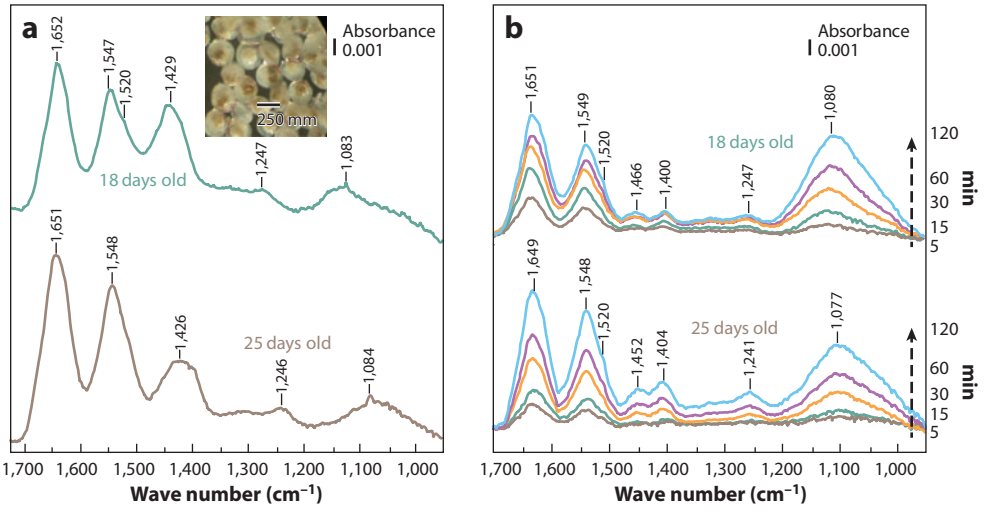

Figure 5

(*a*) Spectra from 18-day-old (*upper*) and 25-day-old (*lower*) mussel larvae (*inset*) on a Ge attenuated total reflectance (ATR) prism, referenced to seawater. (*b*) Spectra of 18-day-old (*upper*) and 25-day-old (*lower*) mussel larvae after 5, 15, 30, 60 and 120 min of settlement time on the Ge ATR prism. Adapted from Reference 23.

major structural component. The peaks at ~1,429 cm^{-1} and ~1,083 cm^{-1} were due to carbonate ion from the mussel larvae shells, whereas the broader peak also centered near 1,080 cm^{-1} was assigned to polysaccharides. The peak near 1,247 cm^{-1} was assigned to the amide III band, which would be expected for glycoproteins, but sulfated polysaccharides could also have contributed in this region. Elemental analysis with EDX confirmed the presence of sulfur (S), indicating that the ~1,247-cm^{-1} band in the IR is probably due to sulfate (24).

Figure 5*b* shows time-dependent spectra of subsequent adhesive deposition, referenced to the spectra in **Figure 5*a***. Particular differences to note in the spectra in **Figure 5*b*** relative to those in **Figure 5*a*** are the absence of the large peak near 1,429 cm^{-1} and the increased relative intensity near 1,080 cm^{-1}. The absence of the peak near 1,429 cm^{-1} was attributed to (*a*) the $CaCO_3$ from the shell being canceled out by the reference spectrum and (*b*) no new $CaCO_3$ being produced in the adhesive. This finding enabled the observation of less intense peaks near 1,450 cm^{-1} and 1,400 cm^{-1}, which were assigned to C-H bending and carboxylate modes, respectively. The increased intensity at 1,080 cm^{-1} was attributed to the increased relative concentration of polysaccharide.

Because mussel adhesive can readily be broken down into its protein components, several studies have utilized these precursor proteins. These studies have been done to understand how the individual proteins behave and to understand the properties of simplified model films. To date, most have been performed with *M. edulis* foot proteins (Mefps), for which six different proteins have been identified (59–61). Baty et al. (12) examined the adsorption of Mefp-1 and Mefp-2 onto polymer coatings by using ATR-FTIR with a flow cell onto polystyrene (PS)- and poly(octadecyl methacrylate) (POMA)-coated Ge elements. The study was done to determine the effects of different surface properties on adsorption, in which PS exhibits aromatic functionality with moderate surface energy and POMA has aliphatic functionality with low surface energy. The surface coverage was estimated from the area of the amide II band. Very different adsorption characteristics for each polymer were observed by FTIR, as well as by AFM and XPS. In the

FTIR experiments, adsorption was monitored with an ATR flow cell. Rinsing the ATR surface afterwards indicated that the adsorption was irreversible. Noticeable effects of surface properties on adsorption profiles and protein structure were identified. Different band intensities and positions in the FTIR spectra were clearly evident, indicating that mussel adhesive proteins can take on different structures depending on surface properties. Although most of these differences in the FTIR spectra were not definitively assigned, angle-dependent XPS suggested that Mefp probably maximized π-π interactions with the PS surface.

5. RAMAN SPECTROSCOPY

Raman spectroscopy is widely used to characterize molecular chemistries through inelastic scattering of light from vibrational energy transitions in molecules. Raman scattering spectroscopy has found considerable use in analyses of biomaterials, primarily due to the commercialization of instrumentation that permits chemical interrogation of micrometer-scale features through optical focusing of the excitation source and scattered light. An added advantage of Raman scattering is its relative insensitivity to absorption by water at visible wavelengths, which enables the analysis of samples in aqueous solutions as well as hydrated or living tissue. Raman systems with two-dimensional mapping capability or confocal optics configurations enable the generation of spatially resolved images with fixed spectral bandwidths or improved depth resolution, respectively.

5.1. Protein Secondary Structure and Side-Chain Vibrational Modes

Raman has a rich history of utility in protein analysis (62–65) and can access both protein or peptide secondary structure and side-chain chemistries (66–71). Secondary structure is observed through vibrational modes of the protein amide band. Of the amide-related vibrational bands, visible Raman spectroscopy is most sensitive to the amide I and amide III modes (72, 73). A principal advantage of Raman spectroscopy in the amide I region is the relatively weak signal intensity of water at $\sim$1,650 cm^{-1}, which reduces the need to use deuterated water (D_2O) to shift the very strong adsorption of water, as observed in IR spectroscopy. The amide III band is more strongly affected by D_2O, which can assist in structural assignment in combination with the amide I band (74), although there remain questions about the structural assignments of this band (75). For silk fibers, the amide III region shows strong correlation with protein secondary structure changes (76). In addition to accessing the amide I and III bands, Raman scattering is sensitive to the ring structures of the amino acid side chains (particularly ring structures such as those found in tyrosine, tryptophan, phenylalanine, and histidine), as well as to sulfur (S) chemistries (S-S, S-C, and S-H) (65).

Resonance-enhancement effects (vibrational modes for molecules in a chromophore with electronic absorption bands that are resonant with the excitation wavelength) assist protein analysis by increasing detection thresholds by up to six orders of magnitude in protein samples (77). Protein secondary structures and some classes of molecules commonly found in marine bioadhesives exhibit resonance Raman enhancement. For example, quinone chemistries—such as those exhibited in the DOPA residues found in mussel adhesive proteins—are known to exhibit resonance Raman effects at visible wavelengths (78–80). For excitation in the UV, the vibrations from protein secondary structure are selectively enhanced (81, 82), aiding structural analyses of protein conformations such as cross-β-amyloid structures (83, 84) implicated in marine and other natural bioadhesives (10, 14, 50, 85–87).

5.2. Raman Analysis of Adhesive Interfaces in Marine Organisms

Raman spectroscopy has been used as one of many complementary biochemical methods (34, 35, 57, 88) and analytical spectroscopies (10, 14, 42, 89, 90) to provide a general analysis of the composition of barnacle cement. For example, Wiegemann et al. (89) have employed IR-excited Raman spectroscopy to probe S-S bonding in barnacle (*Balanus crenatus*) baseplate adhesive. Prior biochemical analyses of barnacle adhesive proteins from various barnacles suggested relatively high cysteine content (33, 34, 36, 37) as well as a high degree of insolubility (34, 36, 37). Consistent with the biochemistry analysis, Berglin & Gatenholm's (43) studies of barnacle adhesive with EDX revealed a strong S signal. Wiegemann et al., however, did not observe evidence for S-S bonding in their Raman spectra. They postulated that the polydimethylsiloxane (PDMS) release substrate the barnacles had been reared on (and removed from for experiments) may have impacted the cross-linking chemistry (91), thereby preventing S-S bonding. We note that Raman S bands are not necessarily as strong in natural bioadhesives (50) as in reference protein spectra of materials with a high–cysteine residue fraction. In situ, performing visible-wavelength Raman of barnacle baseplate chemistry through various optically transparent substrates with differing surface chemistries (e.g., glass, quartz, and release surfaces such as PDMS) could lead to an explanation.

Visible-wavelength Raman spectroscopy has distinct advantages in characterizing mineralized structures found in marine biofoulers. Mineral structures typically exhibit strong Raman signals, and commonly observed calcium carbonate phases such as aragonite, calcite, and vaterite are readily distinguishable from one another. The intensity of these Raman bands, however, can make it difficult to resolve protein contributions to the signal. The use of Raman spectroscopy to evaluate chemical functionalities other than those described above, and the secondary structure of barnacle cements, has not yet been reported.

Raman spectroscopy has been successfully employed to strengthen chemical understanding of mussel adhesion. The presence of DOPA residues suggests quinone tanning (oxidation and cross-linking of phenyls) as a likely mechanism (92). Taylor et al. (80) used visible-wavelength excitation Raman spectroscopy to characterize frozen samples of extracted Mefp1. These authors compared Raman spectra of the proteins at excitation wavelengths of 532 nm and 785 nm to identify resonance-enhanced (62) vibrations. Taylor et al. found significant enhancement of Raman bands in the 500–700-cm^{-1} region, which is associated with Fe-O bonding chemistries, and catechol ring–vibration bands in the 1,100–1,600-cm^{-1} region. This study bolstered the relevance of Fe^{3+} coordination complexes to cross-link mussel proteins. In addition to coordinating with Fe, the DOPA-rich proteins in mussel adhesives may enhance surface adsorption and adhesion. Ooka & Garrell (93) used normal and surface-enhanced Raman spectroscopy (SERS) on gold colloidal nanoparticles to evaluate synthetic peptide mimics of Mefp1 that contained DOPA residues. These authors showed that the peptides absorbed through DOPA residues onto the gold via deprotonation of the DOPA ring.

Confocal Raman microscopy provides a powerful approach to evaluate bioadhesives and surrounding tissue with very high resolution (see, e.g., Reference 94). Waite and coworkers (78, 95) examined various regions of the adhesive plaque and byssus threads of the mussel *M. galloprovincialis*. The threads themselves are composed of collagen-rich proteins (96) that play a role in the remarkable elastic-mechanical properties of the byssal threads (97–99). At least seven proteins have been identified in the byssal plaque chemistry (100); they are located in specific regions of the byssus and plaque and have substantially differing adhesion properties in laboratory studies of adhesion (78). The protective cuticle on the byssal threads is both mechanically robust (101) and chemically distinct with iron-rich surfaces (101, 102). Harrington et al. (95) recently demonstrated that resonance Raman spectroscopy with confocal imaging conditions clearly resolved the spatial

distribution of DOPA-rich proteins and Fe^{3+} complexes for two different mussels (*M. californianus* and *M. galloprovincialis*). **Figure 6** shows Raman spectra (excited at 785 nm) from cross-sectioned cuticle regions of both mussels, along with the corresponding spatially resolved Raman maps of the organic (C-H stretching mode), catechol-metal (C-O-Fe related stretching and bending modes), and catechol ring (C-O/C-C stretching and C-H bending modes) chemistries' distribution. The maps were created through the integration of intensities in three spectral regions to produce a false-color map of the intensity variation locally across the byssus specimen. These results showed that the DOPA-Fe complexes were located at the periphery (surface) of the cuticle and that the DOPA-metal cross-link density was greater in that region as well.

Schmidt et al. (103) used confocal imaging Raman microscopy to investigate the chemistry of cyprid permanent adhesive that remains underneath live, metamorphosed juvenile barnacles. Barnacles were settled on coverslips, allowing the acquisition of Raman spectra through the glass. Maps were created from integration of the band intensities of spectra in the O-H, C=C, amide I, and C-H spectral regions, as well as the fluorescence background, to create pixels in grayscale corresponding to the relative intensity of each band. The experiments were performed before the juvenile barnacles had calcified their baseplates, so no contributions from the $CaCO_3$ peaks were present. This experiment resolved chemical differences between the residual cyprid adhesive pads and the surrounding area, primarily in a decreased OH content (OH stretch: 3,000–3,800 cm^{-1}) relative to the cured cement; quinone chemistries have also been implicated in cyprid attachment adhesives (104, 105). Interestingly, the evidence from this spatially resolved Raman study did not confirm that hypothesis; in fact, the relative fraction of –OH chemistries was lower in the cyprid footprint region. The cyprid attachment points also showed a strong C=C stretching vibration (1,480–1,580 cm^{-1}), which was attributed to carotenoid chemistries. The amide I signal intensities were low across the images, which the authors attributed to the short measurement time.

In situ Raman spectroscopy holds great promise for real-time analyses of the adhesive chemistries of both permanent and temporary bioadhesives. Recently, elegant experiments with imaging SPR have been used to monitor the movement of barnacle cyprids across a surface, as well as to identify regions in which the temporary adhesive has been left behind (as a footprint) (8). Application of in situ Raman microscopy to these regions, in real time, may be possible, particularly if signal-enhancing geometries or chemistries (e.g., SERS) are employed.

The availability of high-spatial resolution Raman instrumentation, in both normal and confocal imaging modes, should lead to further application of chemical spectroscopy, which will increase our understanding of marine adhesives and their curing processes. The primary challenge is the limited signal intensities for visible- and near-IR-wavelength measurements (which makes long collection times necessary), particularly when native protein chemistries do not generate resonance effects like those observed for metal-chelated DOPA chemistries (80, 106) and carotenoids (77). Resonance effects in the UV- or deep-UV-wavelength range may be useful for examining marine bioadhesives, particularly as applied to secondary structure and aromatic moieties (63, 66, 71).

6. CIRCULAR DICHROISM

Far-UV CD is used extensively to estimate protein secondary structure, and it complements FTIR for this purpose. However, the established methods that are most commonly used for estimating secondary structure from CD spectra require that the sample path length and protein concentration be accurately known, given that most CD deconvolution methods developed for analysis of the overlapping spectral features require that the spectra be normalized. This is not an issue for purified proteins in solution, but it poses a problem for solid-state samples. In some particularly well-designed experiments, investigators analyzed surface-adhered monolayers of known polypeptides

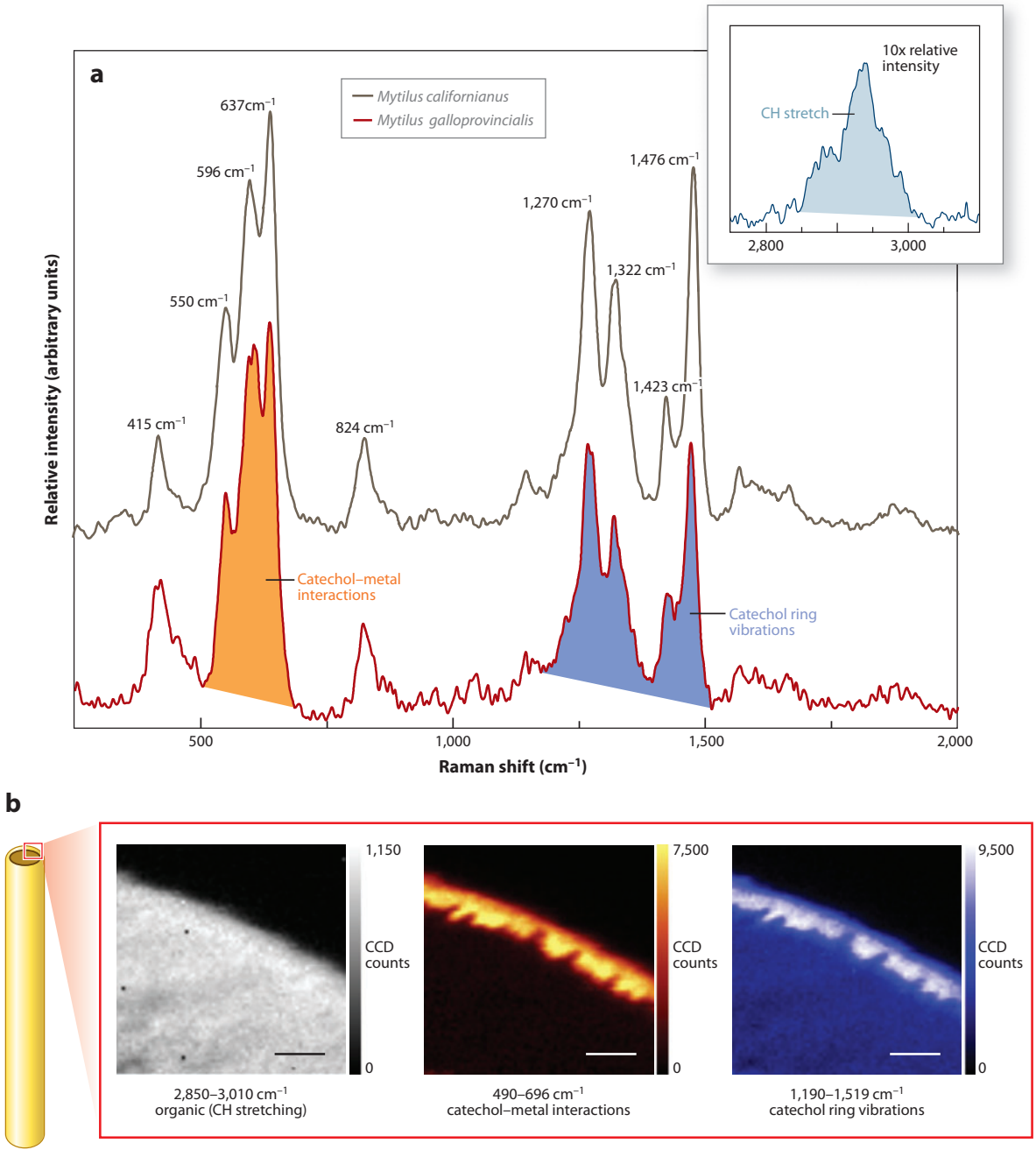

Figure 6

(*a*) Raman spectra of a mussel byssus cuticle from *Mytilus californianus* and *M. galloprovincialis*. The highlighted peaks are attributed to metal-catechol interactions, vibrational modes of carbon in the catechol ring, and (*inset*) C-H stretching modes. (*b*) Spatially resolved image maps from the cuticle end for the three identified chemical regions indicated in panel *a*. The relative intensity of each pixel in a given image represents the integrated signal intensity of the spectral region of interest. Abbreviation: CCD, charge-coupled device. Adapted from Reference 95.

with standard CD deconvolution methods by relying on other methods to normalize the surface concentration (107, 108). Analysis of native, unprocessed bioadhesive films in the solid state require concentration-independent methods of analysis, as with the amide I′ analysis developed by Byler & Susi (48) for FTIR, because the adhesive layer, as formed by the organism, is of nonuniform thickness and consists of an unknown mixture and a concentration of multiple proteins.

Fortunately, methods have been developed for concentration-independent analysis by CD, although they have not yet been extensively applied. Absorption spectra for both CD and UV can be recorded simultaneously, allowing a normalized g-factor spectrum to be obtained by dividing the two. A compilation of g-factor reference spectra and a demonstration of the method through the use of standard deconvolution routines have been reported by McPhie (55, 109, 110) and Baker & Garrell (111). Barlow et al. (10) subsequently employed this g-factor method for an ex situ analysis of barnacle cements in a transmission configuration. The analysis of globular protein structures indicated a higher disordered component, compared with the results from FTIR, but it did confirm β-sheet to be a significant structural component.

SUMMARY POINTS

1. Understanding marine bioadhesion is a complex challenge for which linear optical spectroscopies can be valuable tools. They offer relatively simple yet powerful capabilities for the analysis of bioadhesive films and interfaces, and analyses can be conducted with little or no disruption of the interface. ATR-FTIR in particular has been successfully used to probe the buried adhesive interfaces of live marine organisms.
2. Marine bioadhesive interfaces are often composed of both organic and biomineral components. The FTIR and Raman spectroscopies covered in this review can provide many details about the composition and the biochemical structure of such samples. They can also be applied to observe how these properties change in real time as the live organism adheres to a wet surface.
3. Far-UV CD has also been successfully used to characterize the protein structure of solid-state marine bioadhesive films, and this technique can complement analysis by FTIR and Raman spectroscopies. The use of this method has typically been restricted to the solution state.

FUTURE ISSUES

1. SERS, with or without resonance enhancement, has not been used to examine interfaces in marine adhesion. Local signal enhancements from near-surface regions, or from physically distinct structures, could be examined in situ with appropriate substrates or in vivo with metal nanoparticles.
2. Very little is known about the chemical changes that occur while marine organisms secrete and cure their adhesives. Interfacial approaches that deploy time-resolved and spatially resolved chemical spectroscopy will be essential to determine the curing chemistry and kinetics of marine bioadhesives.

3. Methods to release marine organisms, particularly barnacles, from laboratory substrates often involve PDMS coatings, which have components that may chemically interact with the adhesive. In situ measurements of intact adhesive interfaces, with and without these polymer chemistries, are essential for evaluating chemical interactions between marine organisms and antifouling or release surface treatments.

DISCLOSURE STATEMENT

The authors are not aware of any memberships, affiliations, funding, or financial holdings that might be perceived as affecting the objectivity of this review.

ACKNOWLEDGMENTS

This work was supported by the Office of Naval Research and the basic research program of the Naval Research Laboratory.

LITERATURE CITED

1. Smith AM, Callow JA, eds. 2006. *Biological Adhesives*. Berlin: Springer
2. Waite JH. 1987. Nature's underwater adhesive specialist. *Int. J. Adhes. Adhes.* 7:9–14
3. Dreanno C, Kirby RR, Clare AS. 2006. Smelly feet are not always a bad thing: the relationship between cyprid footprint protein and the barnacle settlement pheromone. *Biol. Lett.* 2:423–25
4. Heydt M, Rosenhahn A, Grunze M, Pettitt M, Callow ME, Callow JA. 2007. Digital in-line holography as a three-dimensional tool to study motile marine organisms during their exploration of surfaces. *J. Adhes.* 83:417–30
5. Rosenhahn A, Schilp S, Kreuzer HJ, Grunze M. 2010. The role of "inert" surface chemistry in marine biofouling prevention. *Phys. Chem. Chem. Phys.* 12:4275–86
6. Bennett SM, Finlay JA, Gunari N, Wells DD, Meyer AE, et al. 2010. The role of surface energy and water wettability in aminoalkyl/fluorocarbon/hydrocarbon-modified xerogel surfaces in the control of marine biofouling. *Biofouling* 26:235–46
7. Cao XY, Pettitt ME, Wode F, Sancet MPA, Fu JH, et al. 2010. Interaction of zoospores of the green alga *Ulva* with bioinspired micro- and nanostructured surfaces prepared by polyelectrolyte layer-by-layer self-assembly. *Adv. Funct. Mater.* 20:1984–93
8. Andersson O, Ekblad T, Aldred N, Clare AS, Liedberg B. 2009. Novel application of imaging surface plasmon resonance for in situ studies of the surface exploration of marine organisms. *Biointerphases* 4:65–68
9. Berglin M, Hedlund J, Fant C, Elwing H. 2005. Use of surface-sensitive methods for the study of adsorption and cross-linking of marine bioadhesives. *J. Adhes.* 81:805–22
10. Barlow DE, Dickinson GH, Orihuela B, Kulp JL, Rittschof D, Wahl KJ. 2010. Characterization of the adhesive plaque of the barnacle *Balanus amphitrite*: Amyloid-like nanofibrils are a major component. *Langmuir* 26:6549–56
11. Aldred N, Phang IY, Conlan SL, Clare AS, Vancso GJ. 2008. The effects of a serine protease, Alcalase®, on the adhesives of barnacle cyprids (*Balanus amphitrite*). *Biofouling* 24:97–107
12. Baty AM, Suci PA, Tyler BJ, Geesey GG. 1996. Investigation of mussel adhesive protein adsorption on polystyrene and poly(octadecyl methacrylate) using angle dependent XPS, ATR-FTIR, and AFM. *J. Colloid Interface Sci.* 177:307–15
13. Dickinson GH, Vega IE, Wahl KJ, Orihuela B, Beyley V, et al. 2009. Barnacle cement: a polymerization model based on evolutionary concepts. *J. Exp. Biol.* 212:3499–510

14. Sullan RMA, Gunari N, Tanur AE, Yuri C, Dickinson GH, et al. 2009. Nanoscale structures and mechanics of barnacle cement. *Biofouling* 25:263–75
15. Waite JH, Tanzer ML. 1981. Polyphenolic substance of *Mytilus edulis*: novel adhesive containing L-dopa and hydroxyproline. *Science* 212:1038–40
16. Lee H, Lee BP, Messersmith PB. 2007. A reversible wet/dry adhesive inspired by mussels and geckos. *Nature* 448:338–41
17. Lee BP, Dalsin JL, Messersmith PB. 2002. Synthesis and gelation of DOPA-modified poly(ethylene glycol) hydrogels. *Biomacromolecules* 3:1038–47
18. Saroyan JR, Lindner E, Dooley CA. 1970. Repair and reattachment in the Balanidae as related to their cementing mechanism. *Biol. Bull.* 139:333–50
19. Cheung PJ, Ruggieri GD, Nigrelli RF. 1977. New method for obtaining barnacle cement in liquid state for polymerization studies. *Mar. Biol.* 43:157–63
20. Dougherty WJ. 1996. Zinc metalloprotease activity in the cement precursor secretion of the barnacle, *Chthamalus fragilis* Darwin. *Tissue Cell* 28:439–47
21. Power AM, Klepal W, Zheden V, Jonker J, McEvilly P, von Byern J. 2010. Mechanisms of adhesion in adult barnacles. In *Adhesion Phenomena in Nature*, ed. J Von Byern, I Grunwald, pp. 153–68. New York: Springer
22. Gao ZH, Bremer PJ, Barker ME, Tan EW, McQuillan AJ. 2007. Adhesive secretions of live mussels observed in situ by attenuated total reflection infrared spectroscopy. *Appl. Spectrosc.* 61:55–59
23. Petrone L, Ragg NLC, McQuillan AJ. 2008. In situ infrared spectroscopic investigation of *Perna canaliculus* mussel larvae primary settlement. *Biofouling* 24:405–13
24. Petrone L, Easingwood R, Barker MF, McQuillan AJ. 2011. In situ ATR-IR spectroscopic and electron microscopic analyses of settlement secretions of *Undaria pinnatifida* kelp spores. *J. R. Soc. Interface* 8:410–22
25. Barth A, Zscherp C. 2002. What vibrations tell us about proteins. *Q. Rev. Biophys.* 35:369–430
26. Le Clair SV, Nguyen K, Chen Z. 2009. Sum frequency generation studies on bioadhesion: elucidating the molecular structure of proteins at interfaces. *J. Adhes.* 85:484–511
27. Burkett JR, Hight LM, Kenny P, Wilker JJ. 2010. Oysters produce an organic-inorganic adhesive for intertidal reef construction. *J. Am. Chem. Soc.* 132:12531–33
28. Yule AB, Walker G. 1987. Adhesion in barnacles. In *Barnacle Biology*, ed. AJ Southward, pp. 389–402. Rotterdam: A.A. Balkema
29. Holm ER, Orihuela B, Kavanagh CJ, Rittschof D. 2005. Variation among families for characteristics of the adhesive plaque in the barnacle *Balanus amphitrite*. *Biofouling* 21:121–26
30. Wendt DE, Kowalke GL, Kim J, Singer IL. 2006. Factors that influence elastomeric coating performance: the effect of coating thickness on basal plate morphology, growth and critical removal stress of the barnacle *Balanus amphitrite*. *Biofouling* 22:1–9
31. Holm ER, Kavanagh CJ, Orihuela B, Rittschof D. 2009. Phenotypic variation for adhesive tenacity in the barnacle *Balanus amphitrite*. *J. Exp. Mar. Biol. Ecol.* 380:61–67
32. Dickinson GH. 2008. *Barnacle cement: a polymerization model based on evolutionary concepts*. PhD thesis. Duke Univ. 193 pp.
33. Naldrett MJ. 1993. The importance of sulfur cross-links and hydrophobic interactions in the polymerization of barnacle cement. *J. Mar. Biol. Assoc. U.K.* 73:689–702
34. Naldrett MJ, Kaplan DL. 1997. Characterization of barnacle (*Balanus eburneus* and *B. cenatus*) adhesive proteins. *Mar. Biol.* 127:629–35
35. Kamino K, Odo S, Maruyama T. 1996. Cement proteins of the acorn barnacle, *Megabalanus rosa*. *Biol. Bull.* 190:403–9
36. Kamino K. 2001. Novel barnacle underwater adhesive protein is a charged amino acid–rich protein constituted by a cys-rich repetitive sequence. *Biochem. J.* 356:503–7
37. Kamino K, Inoue K, Maruyama T, Takamatsu N, Harayama S, Shizuri Y. 2000. Barnacle cement proteins—importance of disulfide bonds in their insolubility. *J. Biol. Chem.* 275:27360–65
38. Griffiths PR, de Haseth JA. 2009. *Fourier Transform Infrared Spectrometry*. Hoboken: Wiley
39. Barth A. 2000. The infrared absorption of amino acid side chains. *Prog. Biophys. Mol. Biol.* 74:141–73

40. Suci PA, Geesey GG. 2001. Use of attenuated total internal reflection Fourier transform infrared spectroscopy to investigate interactions between *Mytilus edulis* foot proteins at a surface. *Langmuir* 17:2538–40
41. Sever MJ, Weisser JT, Monahan J, Srinivasan S, Wilker JJ. 2004. Metal-mediated cross-linking in the generation of a marine-mussel adhesive. *Angew. Chem. Int. Ed.* 43:448–50
42. Barlow DE, Dickinson GH, Orihuela B, Rittschof D, Wahl KJ. 2009. In situ ATR-FTIR characterization of primary cement interfaces of the barnacle *Balanus amphitrite*. *Biofouling* 25:359–66
43. Berglin M, Gatenholm P. 2003. The barnacle adhesive plaque: morphological and chemical differences as a response to substrate properties. *Colloids Surf. B Biointerfaces* 28:107–17
44. Chiovitti A, Heraud P, Dugdale TM, Hodson OM, Curtain RCA, et al. 2008. Divalent cations stabilize the aggregation of sulfated glycoproteins in the adhesive nanofibers of the biofouling diatom *Toxarium undulatum*. *Soft Matter* 4:811–20
45. Bhosle N, Suci PA, Baty AM, Weiner RM, Geesey GG. 1998. Influence of divalent cations and pH on adsorption of a bacterial polysaccharide adhesin. *J. Colloid Interface Sci.* 205:89–96
46. Omoike A, Chorover J. 2004. Spectroscopic study of extracellular polymeric substances from *Bacillus subtilis*: aqueous chemistry and adsorption effects. *Biomacromolecules* 5:1219–30
47. Sangeetha R, Kumar R, Doble M, Venkatesan R. 2010. Barnacle cement: an etchant for stainless steel 316L? *Colloids Surf. B* 79:524–30
48. Byler DM, Susi H. 1986. Examination of the secondary structure of proteins by deconvolved FTIR spectra. *Biopolymers* 25:469–87
49. Fowler DM, Koulov AV, Balch WE, Kelly JW. 2007. Functional amyloid—from bacteria to humans. *Trends Biochem. Sci.* 32:217–23
50. Mostaert AS, Giordani C, Crockett R, Karsten U, Schumann R, Jarvis SP. 2009. Characterisation of amyloid nanostructures in the natural adhesive of unicellular subaerial algae. *J. Adhes.* 85:465–83
51. Kamino K. 2008. Underwater adhesive of marine organisms as the vital link between biological science and material science. *Mar. Biotechnol.* 10:111–21
52. Zandomeneghi G, Krebs MRH, McCammon MG, Fandrich M. 2004. FTIR reveals structural differences between native β-sheet proteins and amyloid fibrils. *Protein Sci.* 13:3314–21
53. Fant C, Hedlund J, Hook F, Berglin M, Fridell E, Elwing H. 2010. Investigation of adsorption and cross-linking of a mussel adhesive protein using attenuated total internal reflection Fourier transform infrared spectroscopy (ATR-FTIR). *J. Adhes.* 86:25–38
54. Sangeetha R, Kumar R, Venkatesan R, Doble M, Vedaprakash L, et al. 2010. Understanding the structure of the adhesive plaque of *Amphibalanus reticulatus*. *Mater. Sci. Eng. C* 30:112–19
55. McPhie P. 2004. CD studies on films of amyloid proteins and polypeptides: quantitative g-factor analysis indicates a common folding motif. *Biopolymers* 75:140–47
56. McQuillan AJ. 2001. Probing solid-solution interfacial chemistry with ATR-IR spectroscopy of particle films. *Adv. Mater.* 13:1034–38
57. Walker G. 1972. Biochemical composition of cement of two barnacle species, *Balanus hameri* and *Balanus crenatus*. *J. Mar. Biol. Assoc. U.K.* 52:429–35
58. Ramsay DB, Dickinson GH, Orihuela B, Rittschof D, Wahl KJ. 2008. Base plate mechanics of the barnacle *Balanus amphitrite*. *Biofouling* 24:109–18
59. Vreeland V, Waite JH, Epstein L. 1998. Polyphenols and oxidases in substratum adhesion by marine algae and mussels. *J. Phycol.* 34:1–8
60. Waite JH, Qin XX. 2001. Polyphosphoprotein from the adhesive pads of *Mytilus edulis*. *Biochemistry* 40:2887–93
61. Waite JH. 2002. Adhesion à la moule. *Integr. Comp. Biol.* 42:1172–80
62. Carey PR. 1988. Raman and resonance Raman spectroscopy. In *Modern Physical Methods in Biochemistry, Part B*, ed. A Neiberger, LM van Deenan, pp. 27–64. Dordrecht: Elsevier
63. Chi ZH, Chen XG, Holtz JSW, Asher SA. 1998. UV resonance Raman-selective amide vibrational enhancement: quantitative methodology for determining protein secondary structure. *Biochemistry* 37:2854–64
64. Tuma R. 2005. Raman spectroscopy of proteins: from peptides to large assemblies. *J. Raman Spectrosc.* 36:307–19

65. Peticolas WL. 1995. Raman-spectroscopy of DNA and proteins. In *Biochemical Spectroscopy*, ed. K Sauer, pp. 389–416. San Diego: Academic
66. Asher SA, Ludwig M, Johnson CR. 1986. UV resonance Raman excitation profiles of the aromatic amino-acids. *J. Am. Chem. Soc.* 108:3186–97
67. Socrates G. 2001. *Infrared and Raman Characteristic Group Frequencies*. Chichester, UK: Wiley
68. Lord RC, Yu NT. 1970. Laser-excited Raman spectroscopy of biomolecules. 1. Native lysozyme and its constituent amino acids. *J. Mol. Biol.* 50:509–24
69. Lord RC, Yu NT. 1970. Laser-excited Raman spectroscopy of biomolecules. 2. Native ribonuclease and α-chymotrypsin. *J. Mol. Biol.* 51:203–13
70. Overman SA, Thomas GJ. 1999. Raman markers of nonaromatic side chains in an α-helix assembly: Ala, Asp, Glu, Gly, Ile, Leu, Lys, Ser, and Val residues of phage *fd* subunits. *Biochemistry* 38:4018–27
71. Rava RP, Spiro TG. 1985. Resonance enhancement in the ultraviolet Raman spectra of aromatic amino acids. *J. Phys. Chem.* 89:1856–61
72. Pelton JT, McLean LR. 2000. Spectroscopic methods for analysis of protein secondary structure. *Anal. Biochem.* 277:167–76
73. Bandekar J. 1992. Amide modes and protein conformation. *Biochim. Biophys. Acta* 1120:123–43
74. Cai SW, Singh BR. 2004. A distinct utility of the amide III infrared band for secondary structure estimation of aqueous protein solutions using partial least squares methods. *Biochemistry* 43:2541–49
75. Weymuth T, Jacob CR, Reiher M. 2010. A local-mode model for understanding the dependence of the extended amide III vibrations on protein secondary structure. *J. Phys. Chem. B* 114:10649–60
76. Monti P, Taddei P, Freddi G, Asakura T, Tsukada M. 2001. Raman spectroscopic characterization of *Bombyx mori* silk fibroin: Raman spectrum of silk. *J. Raman Spectrosc.* 32:103–7
77. Efremov EV, Ariese F, Gooijer C. 2008. Achievements in resonance Raman spectroscopy: review of a technique with a distinct analytical chemistry potential. *Anal. Chim. Acta* 606:119–34
78. Hwang DS, Zeng HB, Masic A, Harrington MJ, Israelachvili JN, Waite JH. 2010. Protein- and metal-dependent interactions of a prominent protein in mussel adhesive plaques. *J. Biol. Chem.* 285:25850–58
79. Holten-Andersen N, Mates TE, Toprak MS, Stucky GD, Zok FW, Waite JH. 2009. Metals and the integrity of a biological coating: the cuticle of mussel byssus. *Langmuir* 25:3323–26
80. Taylor SW, Chase DB, Emptage MH, Nelson MJ, Waite JH. 1996. Ferric ion complexes of a DOPA-containing adhesive protein from *Mytilus edulis*. *Inorg. Chem.* 35:7572–77
81. Schweitzer-Stenner R. 2005. Structure and dynamics of biomolecules probed by Raman spectroscopy. *J. Raman Spectrosc.* 36:276–78
82. Schweitzer-Stenner R. 2001. Visible and UV-resonance Raman spectroscopy of model peptides. *J. Raman Spectrosc.* 32:711–32
83. Lednev IK, Shashilov V, Xu M. 2009. Ultraviolet Raman spectroscopy is uniquely suitable for studying amyloid diseases. *Curr. Sci.* 97:180–85
84. Xu M, Shashilov V, Lednev IK. 2007. Probing the cross-β core structure of amyloid fibrils by hydrogen-deuterium exchange deep ultraviolet resonance Raman spectroscopy. *J. Am. Chem. Soc.* 129:11002–3
85. Nakano M, Shen JR, Kamino K. 2007. Self-assembling peptide inspired by a barnacle underwater adhesive protein. *Biomacromolecules* 8:1830–35
86. Mostaert AS, Higgins MJ, Fukuma T, Rindi F, Jarvis SP. 2006. Nanoscale mechanical characterisation of amyloid fibrils discovered in a natural adhesive. *J. Biol. Phys.* 32:393–401
87. Mostaert AS, Jarvis SP. 2007. Beneficial characteristics of mechanically functional amyloid fibrils evolutionarily preserved in natural adhesives. *Nanotechnology* 18:044010
88. Urushida Y, Nakano M, Matsuda S, Inoue N, Kanai S, et al. 2007. Identification and functional characterization of a novel barnacle cement protein. *FEBS J.* 274:4336–46
89. Wiegemann M, Kowalik T, Hartwig A. 2006. Noncovalent bonds are key mechanisms for the cohesion of barnacle (*Balanus crenatus*) adhesive proteins. *Mar. Biol.* 149:241–46
90. Berglin M, Gatenholm P. 1999. The nature of bioadhesive bonding between barnacles and fouling-release silicone coatings. *J. Adhes. Sci. Technol.* 13:713–27
91. Wiegemann M, Watermann B. 2004. The impact of desiccation on the adhesion of barnacles attached to non-stick coatings. *Biofouling* 20:147–53

92. Waite JH. 1990. The phylogeny and chemical diversity of quinone-tanned glues and varnishes. *Comp. Biochem. Physiol. B* 97:19–29
93. Ooka AA, Garrell RL. 2000. Surface-enhanced Raman spectroscopy of DOPA-containing peptides related to adhesive protein of marine mussel, *Mytilus edulis*. *Biopolymers* 57:92–102
94. Caspers PJ, Lucassen GW, Carter EA, Bruining HA, Puppels GJ. 2001. In vivo confocal Raman microspectroscopy of the skin: noninvasive determination of molecular concentration profiles. *J. Investig. Dermatol.* 116:434–42
95. Harrington MJ, Masic A, Holten-Andersen N, Waite JH, Fratzl P. 2010. Iron-clad fibers: a metal-based biological strategy for hard flexible coatings. *Science* 328:216–20
96. Waite JH, Vaccaro E, Sun CJ, Lucas JM. 2002. Elastomeric gradients: a hedge against stress concentration in marine holdfasts? *Philos. Trans. R. Soc. Lond. Ser. B* 357:143–53
97. Gosline J, Lillie M, Carrington E, Guerette P, Ortlepp C, Savage K. 2002. Elastic proteins: biological roles and mechanical properties. *Philos. Trans. R. Soc. Lond. Ser. B* 357:121–32
98. Bell EC, Gosline JM. 1996. Mechanical design of mussel byssus: material yield enhances attachment strength. *J. Exp. Biol.* 199:1005–17
99. Waite JH, Lichtenegger HC, Stucky GD, Hansma P. 2004. Exploring molecular and mechanical gradients in structural bioscaffolds. *Biochemistry* 43:7653–62
100. Zhao H, Sagert J, Hwang DS, Waite JH. 2009. Glycosylated hydroxytryptophan in a mussel adhesive protein from *Perna viridis*. *J. Biol. Chem.* 284:23344–52
101. Holten-Andersen N, Zhao H, Waite JH. 2009. Stiff coatings on compliant biofibers: the cuticle of *Mytilus californianus* byssal threads. *Biochemistry* 48:2752–59
102. Sun CJ, Waite JH. 2005. Mapping chemical gradients within and along a fibrous structural tissue: mussel byssal threads. *J. Biol. Chem.* 280:39332–36
103. Schmidt M, Cavaco A, Gierlinger N, Aldred N, Fratzl P, et al. 2009. In situ imaging of barnacle (*Balanus amphitrite*) cyprid cement using confocal Raman microscopy. *J. Adhes.* 85:139–51
104. Okano K, Shimizu K, Satuito CG, Fusetani N. 1996. Visualization of cement exocytosis in the cypris cement gland of the barnacle *Megabalanus rosa*. *J. Exp. Biol.* 199:2131–37
105. Phang IY, Aldred N, Clare AS, Callow JA, Vancso GJ. 2006. An in situ study of the nanomechanical properties of barnacle (*Balanus amphitrite*) cyprid cement using atomic force microscopy (AFM). *Biofouling* 22:245–50
106. Masic A, Harrington M, Waite JH, Fratzl P. 2010. In situ Raman sectroscopic imaging of a mussel coating and adhesive. *Proc. Int. Conf. Raman Spectrosc.*, pp. 358–59
107. Sivaraman B, Fears KP, Latour RA. 2009. Investigation of the effects of surface chemistry and solution concentration on the conformation of adsorbed proteins using an improved circular dichroism method. *Langmuir* 25:3050–56
108. Fears KP, Latour RA. 2009. Assessing the influence of adsorbed-state conformation on the bioactivity of adsorbed enzyme layers. *Langmuir* 25:13926–33
109. McPhie P. 2001. Circular dichroism studies on proteins in films and in solution: estimation of secondary structure by g-factor analysis. *Anal. Biochem.* 293:109–19
110. McPhie P. 2008. Concentration-independent estimation of protein secondary structure by circular dichroism: a comparison of methods. *Anal. Biochem.* 375:379–81
111. Baker BR, Garrell RL. 2004. g-Factor analysis of protein secondary structure in solutions and thin films. *Faraday Discuss.* 126:209–22

Annual Review of
Analytical Chemistry

Volume 5, 2012

Contents